Biomedical Analysis 1 (2024) 103–110

Contents lists available at ScienceDirect

Biomedical Analysis

journal homepage: www.keaipublishing.com/en/journals/bioana/

Engineered exosome-based drug delivery system for synergistic cancer therapy via autophagy inhibition and chemotherapy

Xin Hua[a], Yu Liu[a], Xi Liu[a], Qian Zhu[a], Sisi Zhou[a], Quan Li[b], Songqin Liu[a,*]

[a] Jiangsu Engineering Laboratory of Smart Carbon-Rich Materials and Device, School of Chemistry and Chemical Engineering, Southeast University, Nanjing 211189, China
[b] College of Chemistry and Materials Science, Sichuan Normal University, Chengdu 610068, China

ARTICLE INFO

Keywords:
Exosomes
Drug delivery
Synergistic therapy
Ovarian cancer

ABSTRACT

Exosomes (EXOs) are a class of natural nanovesicles secreted endogenously by mammalian cells. Recent decades have witnessed the broad applications of exosomes in cancer diagnosis and treatment. In the present study, an exosome-based drug delivery system employing synergistic miRNA-based autophagy inhibition and 7-coumarin-based chemotherapy was established for ovarian cancer therapy. Taking advantage of the outstanding biocompatibility and immune evasion, exosomes are used as carriers for targeted drug delivery. Magnetic nanoparticles (MNPs) were coupled to exosomes to improve the separation efficiency of exosomes. Two drugs, miRNA-FAM and 7-coumarin, were loaded into EXOs-MNPs by electroporation to achieve the miRNA-FAM/7-coumarin@EXOs-MNPs drug delivery system. The engineered exosome-based drug delivery system improved the cell entry ability of drugs and the targeting of cancer cells. Simultaneous application of the two drugs significantly improved the efficacy of cancer cell therapy, indicating that the two drugs have synergistic effects. Therefore, this work provided a new drug delivery system and synergistic therapy idea, which showed great potential for future clinical applications.

1. Introduction

Ovarian cancer is one of the most common malignancies in women worldwide. Unlike breast cancer, ovarian cancer lacks early diagnostic markers and does not show noticeable symptoms until cancer metastases, leading to a low survival rate for ovarian cancer patients [1]. Therefore, the treatment of ovarian cancer remains a challenge. Traditional cancer treatments include surgery, radiation therapy, chemotherapy and interventional therapy. However, the distribution of chemotherapeutic drugs in vivo is non-specific and often toxic to healthy cells, leading to unsatisfactory efficacy [2,3]. With the development of precision medicine, targeted therapy and immunotherapy are gradually applied to the treatment of cancer, especially advanced cancer.

Exosomes are extracellular vesicles with lipid bilayers (30–150 nm in diameter) that are secreted by most cells in the body. They are widely present in various body fluids, carrying and transmitting important signaling molecules. In recent years, exosomes have been extensively used as delivery vehicles for multiple drugs due to their high biocompatibility, low immunogenicity, the abilities to cross various biological barriers and evade the clearance by immune system [4–6]. Inspired by this, an increasing number of research focus on exosome-based drug delivery systems [7–10]. The delivered drugs mainly include small molecular drugs and biomolecular

* Corresponding author.
E-mail address: liusq@seu.edu.cn (S. Liu).

https://doi.org/10.1016/j.bioana.2024.05.002
Received 29 April 2024; Received in revised form 24 May 2024; Accepted 24 May 2024

drugs, such as chemotherapeutic drugs, proteins, peptides, mRNAs, miRNAs, siRNAs, etc. The use of various nucleic acids could regulate the expression of cancer development-related genes and thereby play a therapeutic role [11–14]. Recently, multi-drug-loaded exosome-based drug delivery systems for synergistic cancer therapy have been reported. Du et al. [15] obtained CD47-overexpressing exosomes and loaded iron death inducer (erastin, Er) and PS (rose Bengal, RB) into them by ultrasound. Under laser irradiation, tumor cell death was synergistically induced by the iron death effect of Er and photodynamic therapy (PDT) of RB, resulting in enhanced liver cancer treatment effect with lower liver and kidney toxicity. Yuan et al. [16] loaded chemotherapeutic drug doxorubicin (DOX)-modified iron oxide nanoparticles into 4T1 mouse breast cancer cell-derived exosomes. The system could be used for combined therapy including photothermal and chemotherapeutic treatment under laser irradiation. Over all, synergistic cancer treatment utilizes the advantages of different therapeutic approaches and has been applied to effectively treat cancers through the synergy of different treatment mechanisms. Besides, synergistic treatment with nanomaterial systems can significantly reduce the dose of anti-cancer drugs required and the toxic side effects, and meanwhile increase drug delivery targeting [17,18].

Autophagy is an intracellular degradative process where a cell engulfs its own cytoplasmic proteins or organelles and encapsulates them into autophagosomes. The autophagosomes then fuses with lysosomes to form double-membraned vesicles that degrade their contents, leading to fulfilling the cell's own metabolic needs and providing energy and macromolecular precursor [19,20]. Many studies have shown that in cancer biology, autophagy plays a dual role in tumor promotion and inhibition [21]. A large number of clinical evidence supports the opinion that inhibition of autophagy improves the clinical treatment of cancer patients [22,23]. Chloroquine (CQ) and hydroxychloroquine (HCQ) are the only two clinical agents currently available for the inhibition of autophagy. These drugs deacidify lysosomes and prevent the fusion of autophagosomes with lysosomes, thereby inhibiting autophagy [24]. In addition, a small trial involving 18 patients with glioblastoma provided the first clinical evidence of improved prognosis through the utilization of autophagy inhibition. Patients treated with CQ in combination with radiotherapy and temozolomide had a significantly longer median survival compared to the control group (33 months vs. 11 months) [25]. The results of the initial study were supported by follow-up clinical trials and retrospective data from Briceno et al. [26,27]. Other early studies of CQ in combination with radiotherapy for brain metastases also resulted in improved control of intracranial tumors. In addition, genetically engineered mouse models (GEMMs) and patient-derived xenograft (PDX) mouse models have shown evident antitumor effects when treated with various types of anticancer agents in combination with autophagy inhibition [19,28].

Based on this, we elaborately constructed a novel antitumor exosome-based drug delivery system employing the synergistic effects of miRNA-regulated autophagy inhibition and coumarin anticancer drugs to achieve effective treatment of ovarian cancer. The excellent drug activity and the unique optical properties of the 7-coumarin could be used to achieve anti-tumor effects and intracellular visualization. At the same time, the encapsulated miRNA can participate in the regulation of the autophagy process, reducing autophagic flux and inhibiting the proliferation and activity of cancer cells. Both of the two anticancer active molecules were encapsulated into exosomes through electroporation. In addition, magnetic nanobeads were modified on the surface of exosomes through the specific interactions between transferrin (Tf) and transferrin receptors (TfR) to facilitate efficient separation and enrichment of exosome-based drug delivery systems.

2. Experimental section

2.1. Chemicals and materials

Fetal bovine serum (FBS), Dulbecco's Modified Eagle Medium (DMEM), RPMI-1640 medium and phosphate-buffered saline (PBS, 0.1 M, pH 7.4) were purchased from KeyGen Biotechnology (Nanjing, China). Bicinchoninic Acid (BCA) protein quantitation assay kits, Annexin V-FITC/PI apoptosis assay kits, and 3-(4, 5-dimethylthiazol-2-yl)-2, 5-diphenyl-tetrazolium bromide (MTT) were obtained from Sangon Biotechnology (Shanghai, China). Carboxylated chitosan (CS) was purchased from Beijing Jinming Biotechnology (Beijing, China). 7-Coumarin was received from Shanghai Yuanmu Biotechnology (Shanghai, China). N-hydroxysuccinimide (NHS) and 1-ethyl-3-(3'-dimethyl aminopropyl) carbodiimide (EDC) were purchased from Thermo Fisher Inc. (Shanghai, China). Ammonia was purchased from Shanghai Macklin Biotechnology (Shanghai, China). Dialysis bags were purchased from Shanghai Baoman Biotechnology (Shanghai, China). Transferrin (Tf) was purchased from Sigma-Aldrich (USA). The sequences of miRNA-129 oligonucleotides with fluorescent dye (FAM) linked to its 5' terminal (5'-FAM-CUUUUUGCGGUCUGGGCUUGC) were synthesized by Sangon Biotechnology (Shanghai, China). Hexahydrate ferric chloride ($FeCl_3{\cdot}6H_2O$), tetrahydrate ferrous chloride ($FeCl_2{\cdot}4H_2O$), and other chemical reagents were purchased from Aladdin Reagent (Shanghai, China) and used as received. Deionized water (Millipore Milli-Q grade) with a resistivity of 18.2 MΩ cm was used in all the experiments.

2.2. Instruments

The morphology and structure of the vesicles were characterized by Transmission Electron Microscope (TEM, JEM-2010, JEOL, Japan), Scanning Electron Microscope (SEM, JSM-7001F, JEOL, Japan), and Confocal Laser Scanning Microscopy (CLSM, FluoView™ FV1000, Olympus, Japan). Fluorescence spectra were carried out on a FluoroMax-4 Spectrofluorometer with Xenon discharge lamp excitation (HORIBA, Japan). The zeta potentials were measured at 25 °C on a Malvern Zetasizer NanoZS instrument (UK). The absorbance values of MTT were recorded by a Safire2 microplate reader (Thermo Fisher Scientific, USA). Exosomes were collected using an ultracentrifuge (Optima XE-90, Beckman Coulter, USA). The concentration and size distribution of exosomes were measured by Nanoparticle Tracking Analysis (NTA, NanoSight NS300, Malvern Panalytical, UK). Drug was loaded into the exosomes by electroporation using an electroporation system (Gene Pulser, Bio-Rad, USA).

2.3. Cell culture and exosomes collection

The cells used in this work were obtained from the cell bank of type culture collection of the Chinese Academy of Sciences in Shanghai. Human Ovarian cancer cells (SKOV-3) and human normal ovarian epithelial cells (IOSE80) were incubated in the DMEM culture medium and RPMI 1640 culture medium, respectively. All culture media were supplied with FBS (10 %), streptomycin (100 mg/mL), and penicillin (100 U/mL). All cells were cultured in a 37 ℃ incubator with a 5 % CO_2 atmosphere.

To collect exosomes, the cells were cultured in a serum-free culture medium for about 48 h. After the growth reached 80 %, exosomes were harvested and separated from the supernatant by centrifugation. Briefly, the cell debris was first eliminated from the conditioned medium by centrifugation for 10 min (RCF = 2000 *g*). The supernatant was further centrifuged for 30 min at 4 ℃ (RCF = 10,000 *g*) to remove other impurities. Then, the supernatant was collected and ultracentrifuged at 4 ℃ for 70 min (RCF = 100,000 *g*). After washing three times with PBS, exosomes were resuspended in PBS and stored at − 80 ℃ for later use.

2.4. Preparation and modification of EXOs-MNPs

MNPs were synthesized by a typical chemical co-precipitation reaction of Fe^{2+} and Fe^{3+} in ammonium hydroxide solution according to the following reaction:

$$2FeCl_3 + FeCl_2 + 8NH_3{\cdot}H_2O = Fe_3O_4 + 8NH_4Cl + 4H_2O$$

In brief, 5 mL $FeCl_3{\cdot}6H_2O$ (2.5 mol L^{-1}) was mixed with 8.75 mL $FeCl_2{\cdot}4H_2O$ (2.5 mol L^{-1}) at pH 5.5. 10 mL CS (0.8 mg mL^{-1}) was added to the mixture. The pH value was then adjusted to 10. After that, the mixture was placed in a water bath heated to 80 ˚C in advance and stirred for 1 h. After the reaction, the solution was cooled to room temperature and dialyzed in deionized water for 48 h. The water was replaced every 6 h to obtain CS-modified magnetic ferric tetroxide nanoparticles (MNPs-CS) by desalting.

MNPs-CS (1 mg mL^{-1}) were mixed with EDC and NHS at a molar ratio of 1: 2: 3 (pH 5.5). This mixture was incubated at room temperature for 1 h. Then, the reaction was terminated by adding 5-mercaptoethanol. Activated MNPs-CS were washed with PBS for three times and resuspended in PBS (pH = 7.4). After that, 10 μg of Tf was added into the solution and incubated at 4 ˚C for 12 h. Finally, the MNPs-Tf were obtained by magnetic separation and washed with PBS for three times, which was stored at 4 ˚C for future use.

To prepare EXOs-MNPs, MNPs-Tf were mixed with exosomes and incubated at 4 ˚C for 4 h. This allowed MNPs-Tf to be coated onto exosomes by Tf-TfR interaction. After that, unreacted exosomes were removed by magnetic separation.

2.5. Drug loading

MiRNA-FAM and 7-coumarin were loaded into exosomes by electroporation. In order to simplify quantification, the protein concentration of EXOs-MNPs was measured by BCA assay and was used to represent the mass concentration of EXOs-MNPs during electroporation. In this way, EXOs-MNPs and miRNA-FAM/7-coumarin were mixed in PBS at a mass ratio of 1:1. The concentration of EXOs-MNPs in the mixture was 0.5 mg mL^{-1}. 600 μL of the mixture was added to the electric converter, while the electroporation system was set up at 400 mV, 125 μF with a pulse time of 10 ms. At the end of the procedure, the unreacted miRNA-FAM and 7-coumarin in the supernatant were removed by magnetic separation. The resulting material was re-dispersed in PBS and allowed to stand at 4 ℃ for 30 min to obtain miRNA-FAM/7-coumarin@EXOs-MNPs. For comparison, single-loaded miRNA-FAM@EXOs-MNPs and 7-coumarin@EXOs-MNPs were prepared following the same procedure with only one drug used.

The loading efficiency of miRNA-FAM and 7-coumarin by electroporation was determined by comparing the fluorescence intensities of miRNA-FAM and 7-coumarin before and after electroporation.

2.6. Cell viability

MTT assay was employed to detect the toxicity of synthesized materials. To be specific, IOSE80 cells or SKOV-3 cells were seeded in 96-well plates at a density of about 10^5 cells per well. The plates were incubated at 37 ˚C for 12 h. After being treated with PBS, synthesized materials with gradient concentrations were added. After 24 h of incubation, carefully aspirate the culture medium, and 200 μL (500 μg mL^{-1}) MTT was added to each well and further incubated at 37 ˚C for 4 h. Then the excess medium in the well plate was abandoned. 150 μL of dimethyl sulfoxide (DMSO) was added to dissolve the produced formazan by living cells. Finally, the cell plate was vibrated for 15 min at 37 ˚C, and the absorbance at a wavelength of 490 nm (OD-490) was measured to obtain the cell viability calculated by ($OD\text{-}490_{sample}/OD\text{-}490_{control}$) × 100 %.

2.7. Anticancer efficacy study in vitro

The anticancer efficacy of the synthesized materials was investigated using the Annexin V-FITC/PI Apoptosis Detection Kit (BD Biosciences) by flow cytometry. SKOV-3 cells were seeded in 6-well plates at a density of approximately 10^6 cells per well and cultured in a 2 mL DMEM medium for 12 h. Then, 20 μg EXOs-MNPs, 20 μg miRNA-FAM@EXOs-MNPs, 20 μg 7-coumarin@EXOs-MNPs, 20 μg miRNA-FAM/7-coumarin@EXOs-MNPs, 40 μg miRNA-FAM/7-coumarin@EXOs-MNPs, and 60 μg miRNA-FAM/7-coumarin@EXOs-MNPs were added, respectively. After 8 h, the cells were digested and collected, and then stained with the Annexin V-

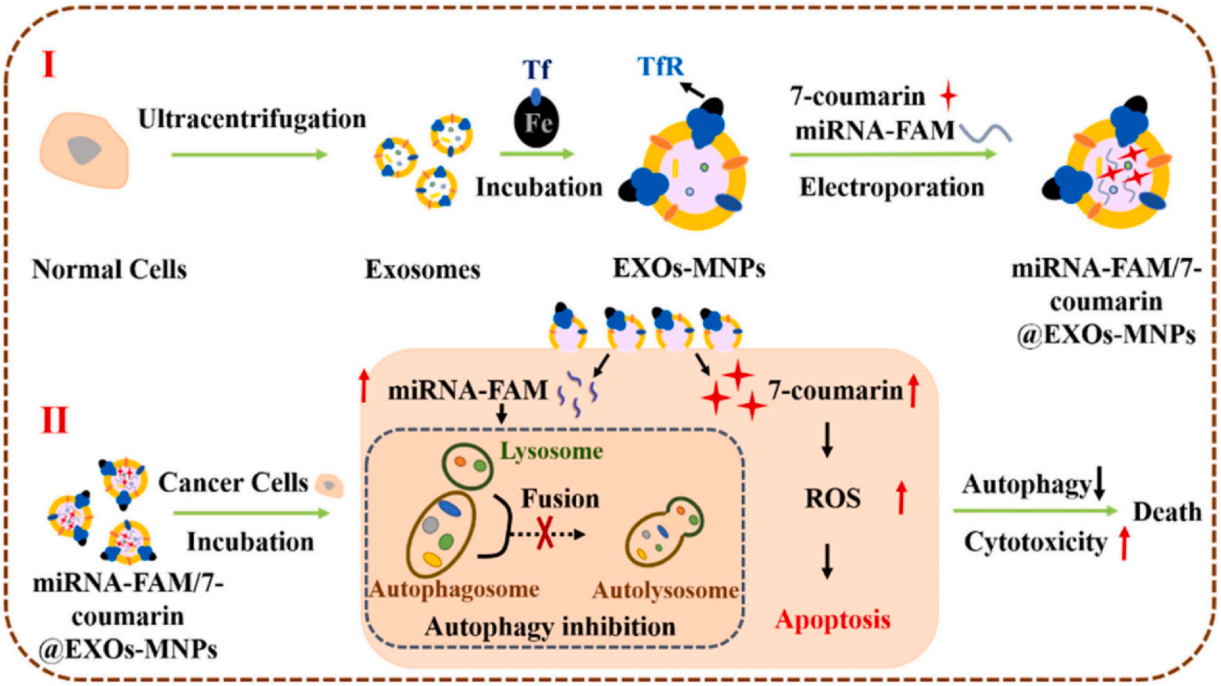

Fig. 1. Schematic diagram of (I) the preparation and (II) the synergetic cancer therapy of miRNA-FAM/7-coumarin@EXOs-MNPs drug delivery system.

FITC/PI cell assay kit following manufacturer's instructions. Finally, the cell apoptosis and necrosis in each sample were analyzed by the BD FACS Calibur Flow Cytometer following the manufacturer's protocol.

3. Results and discussion

The designed miRNA-FAM/7-coumarin@EXOs-MNPs drug delivery system was shown in Fig. 1. Exosomes secreted by the IOSE80 cells were employed as carriers to load two drugs including 7-coumarin and miRNA-FAM. MNPs were decorated with transferrin (Tf) to specifically bind with the transferrin receptor (TfR) on the surface of exosomes to form miRNA-FAM/7-coumarin@EXOs-MNPs (**Step I**). Upon taking up by tumor cells (**Step II**), the miRNAs inhibited the proliferation and activity of cancer cells by regulating autophagy, while 7-coumarin exerted its anti-cancer effects to kill cancer cells. Thus, synergistically effective treatment of ovarian cancer was achieved.

3.1. Construction and characterization of miRNA-FAM/7-coumarin@EXOs-MNPs

MNPs are usually superparamagnetic at sizes smaller than 25 nm. TEM, SEM and dynamic light scattering (DLS) analysis showed that the prepared MNPs were spherical with uniform particle size of about 13 nm (Fig. S1). MNPs were dispersed and stabilized in PBS solution. However, the applied magnetic field can cause rapid accumulation of MNPs, indicating that MNPs have good magnetic properties (Fig. S2A). After being crosslinked with Tf via amine-carboxylic acid, MNPs-Tf maintained good dispersion and magnetic field response (Fig. S2B). The protein loading per mg of MNPs was 20.6 μg by the BCA method.

Exosomes were collected by ultracentrifugation from cell supernatants and characterized by TEM, NTA and Western blot (Fig. S3). The mean diameter of the collected exosomes detected by DLS was 116 nm, while the mean diameter of the EXOs-MNPs increased slightly by 15 nm (Fig. S4A). TEM images showed dark spots around spherical vesicles, which provided direct visual evidence for the formation of EXOs-MNPs (Fig. S4B). BCA experiments show that when MNPs-Tf binds to exosomes, the amount of protein in MNPs gradually increases (Fig. S5A–B). EXOs-MNPs showed good storage stability and no obvious aggregation was observed after 7 days in PBS buffer at 4 °C (Fig. S5C).

Frequently used exogenous drug loading strategies for exosomes include direct incubation, electroporation, sonication, extrusion [29], etc. Direct incubation is the simplest method. However, for hydrophilic drugs such as RNA, a major obstacle was formed by the lipid bilayer membrane of exosomes, which severely limited the passive loading of RNAs. In electroporation, by applying an electrical signal with a certain voltage, tiny pores can be spontaneously formed in membranes, which has been proven to be suitable for RNA loading [30]. Therefore, the exosomes were loaded with 7-coumarin and miRNA by electroporation. By measuring the fluorescence intensity of the solution before and after electroporation, the encapsulation efficiencies of miRNA-FAM and 7-coumarin in exosomes were calculated to be 18.6 % and 21.7 %, respectively (Fig. S6). Flow cytometry analysis showed clear FAM (green) channels, confirming that miRNA-FAM have been successfully encapsulated into exosomes (Fig. S7).

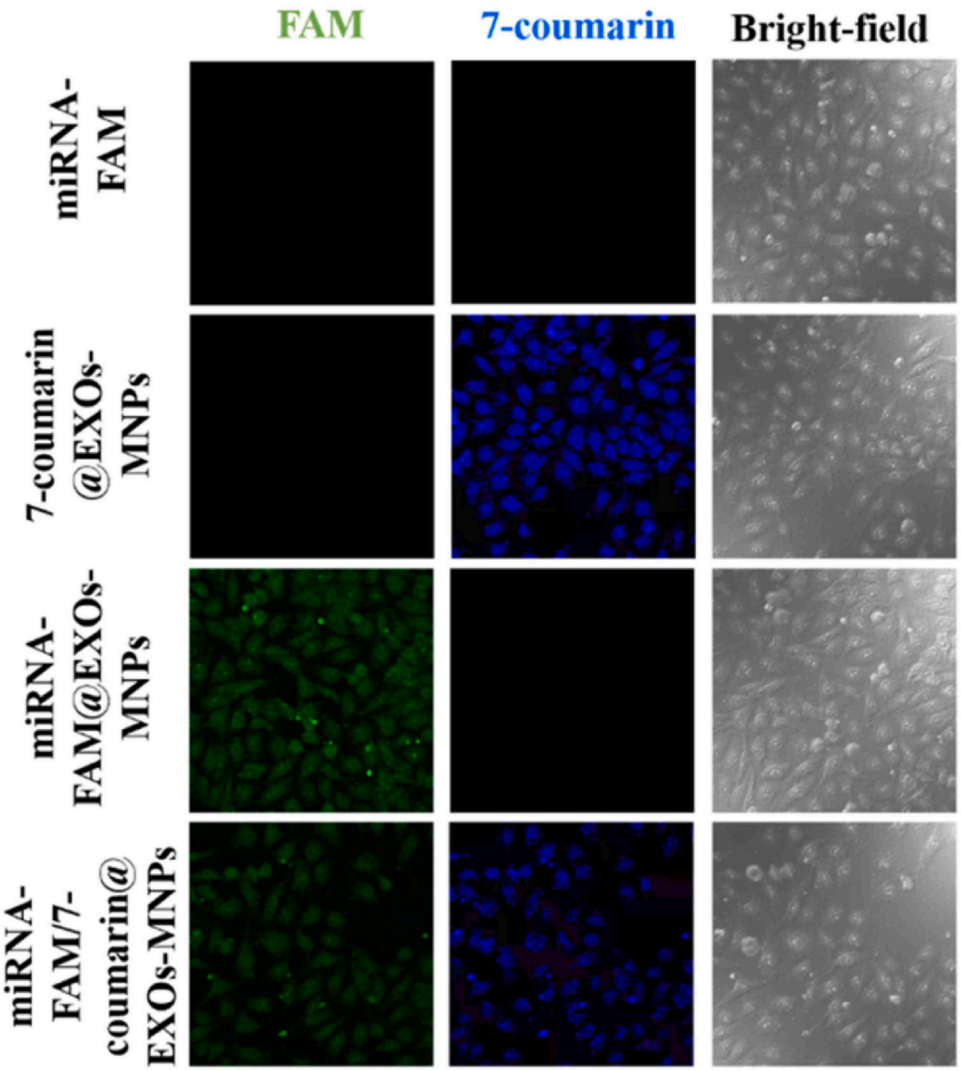

Fig. 2. CLSM images of different materials co-incubated with IOSE80 cells for 8 h.

3.2. Cytotoxicity and cell-uptaking of different material

The cell-uptaking properties of different materials were observed by confocal microscopy. After IOSE80 cells were co-incubated with miRNA-FAM or 7-coumarin for 8 h, almost no green or blue fluorescence was observed in the target cells (Fig. 2). This was due to the hydrophilic and negatively charged properties of miRNA or 7-coumarin, which were difficult to directly cross the cell membrane into the cell. When IOSE80 cells were treated with miRNA-FAM@EXOs-MNPs or 7-coumarin@EXOs-MNPs, clear green or blue fluorescence was observed in FAM or 7-coumarin channels, respectively, suggesting that exosomes could enhance cell drug uptaking through homologous targeting interactions. For miRNA-FAM/7-coumarin@EXOs-MNPs treated cells, clear blue and green fluorescence could be simultaneously observed in both 7-coumarin and FAM channels, which confirmed that miRNA and 7-coumarin were successfully encapsulated in exosomes and entered cells smoothly. The time-dependent cell-uptaking showed that the number of miRNA-FAM/7-coumarin@EXOs-MNPs uptaking by the target cells gradually increased with the increase of incubation time, especially during the first 4 hours. During 6–8 h, the exosome uptake slowed down and reached an equilibrium (Fig. S8A). CLSM images showed a clear green FAM fluorescence in cells after incubating with miRNA-FAM/7-coumarin@EXOs-MNPs for 2 h. With the increase of incubation time, the fluorescence intensity in cells gradually increased and reached a maximum at 6 h, which demonstrated that most of the miRNA-FAM/7-coumarin@EXOs-MNPs had entered the cells at 6 h (Fig. S8B).

The cytotoxicity of these materials was studied using MTT assay. EXOs-MNPs showed low cytotoxicity with cell viability exceeding 85 % even at EXOs-MNPs concentrations up to 200 μg mL^{-1}. miRNA-FAM@EXOs-MNPs and 7-coumarin@EXOs-MNPs had significant inhibitory activity on cancer cells. The higher the material concentration, the greater the toxicity was observed. At concentration of 20 μg mL^{-1}, the cell-viability of IOSE80 and SKOV-3 cells were approximately 77 % and 70 % for 7-coumarin@EXOs-MNPs and 75 % and 66 % for miRNA-FAM@EXOs-MNPs, respectively. When miRNA-FAM/7-coumarin@EXOs-MNPs was

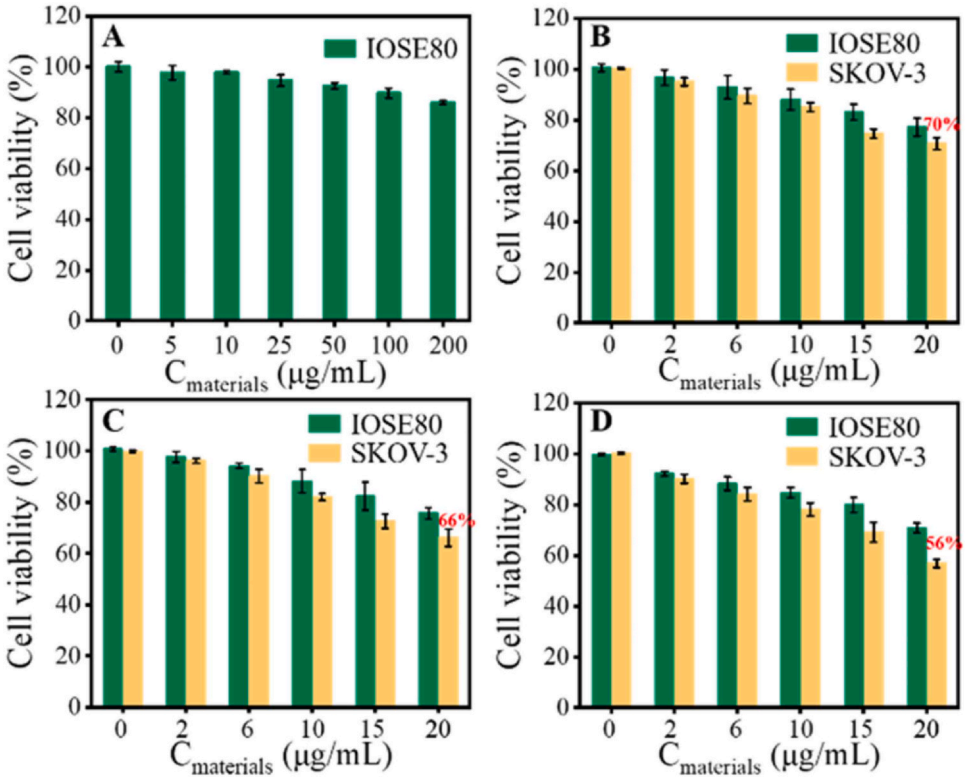

Fig. 3. (A) Cell viability of IOSE80 cells after incubation with different concentrations of EXOs-MNPs under normoxic conditions. Cell viability of IOSE80 and SKOV-3 cells after incubation with different concentrations of (B) 7-coumarin@EXOs-MNPs (C) miRNA-FAM@EXOs-MNPs and (D) miRNA-FAM/7-coumarin@EXOs-MNPs. Data were shown as means ± SD (n = 3).

incubated with cells, the inhibition effect was more pronounced, with a survival rate of less than 56 % for cancer cells at a concentration of 20 μg mL^{-1}. This indicated the synergistic effect of miRNA-FAM/7-coumarin@EXOs-MNPs on cancer cells (Fig. 3).

3.3. Synergistic therapeutic effect of miRNA-FAM/7-coumarin@EXOs-MNPs

An apoptosis kit was further used to verify the synergistic anti-cancer effect of the materials and their concentration-dependent behavior (Fig. 4). The flow cytometry assay showed that all of miRNA-FAM@EXOs-MNPs, 7-coumarin@EXOs-MNPs and miRNA-FAM/7-coumarin@EXOs-MNPs could induce cell apoptosis, but the percentage of apoptosis varied greatly with different materials. The percentage of apoptosis increased significantly from 2.493 % or 7.47 % for single miRNA or 7-coumarin loading to 20.58 % for miRNA-FAM/7-coumarin@EXOs-MNPs. Moreover, the apoptotic effect increased with the concentration of miRNA-FAM/7-coumarin@EXOs-MNPs, and the apoptosis rate reached 49.51 % when 60 μg mL^{-1} miRNA-FAM/7-coumarin@EXOs-MNPs was added.

Chemotherapy is the main treatment for some tumors which tend to disseminate systemically or have metastasized in the middle and late stages. Chemotherapeutic drugs can act on different aspects of tumor cell growth and reproduction, which can achieve the purpose of inhibition or treatment by inducing apoptosis of cancer cells. However, tumor cells often escape apoptosis through autophagy, thus reducing the efficacy of chemotherapy. In the past decade, it was widely believed that inhibition of autophagy played a role in promoting the efficacy of chemotherapy. Data from several experiments have shown that autophagy inhibitors such as 3-methyladenine, worman penicillin, chloroquine or hydroxychloroquine can enhance the therapeutic effects of drugs with pharmacological autophagy-inhibiting activity when combined with other conventional chemotherapeutic drugs [31,32]. In this work, an miRNA (miR-129) was used to block the fusion between autophagosomes and lysosomes in the autophagy procedure, and therefore inhibit autophagy. In addition, 7-coumarin was used to produce ROS and accelerate the apoptosis of cancer cells. From the results, it was clear that simultaneously employing the two drugs achieved a significantly better therapeutic effect than using single drugs, demonstrating the synergistic effect of the two drugs. One drawback of the current drug delivery system is the targeting of the system towards cancerous cells. As shown in Figs. 2 and 3, the system could also enter and kill normal cells (IOSE80). However, encapsulating the drugs into exosomes enhanced the cell-entering capability of the drugs and to some extent increased the targeting of the drugs to cancer cells (Fig. 3). In our future work, more targeting molecules such as antibodies or aptamers will be modified to the system and are expected to significantly enhance the targeting ability of the system toward cancer cells. Therefore, the exosome-based drug delivery system provides a promising new idea and approach for cancer treatment.

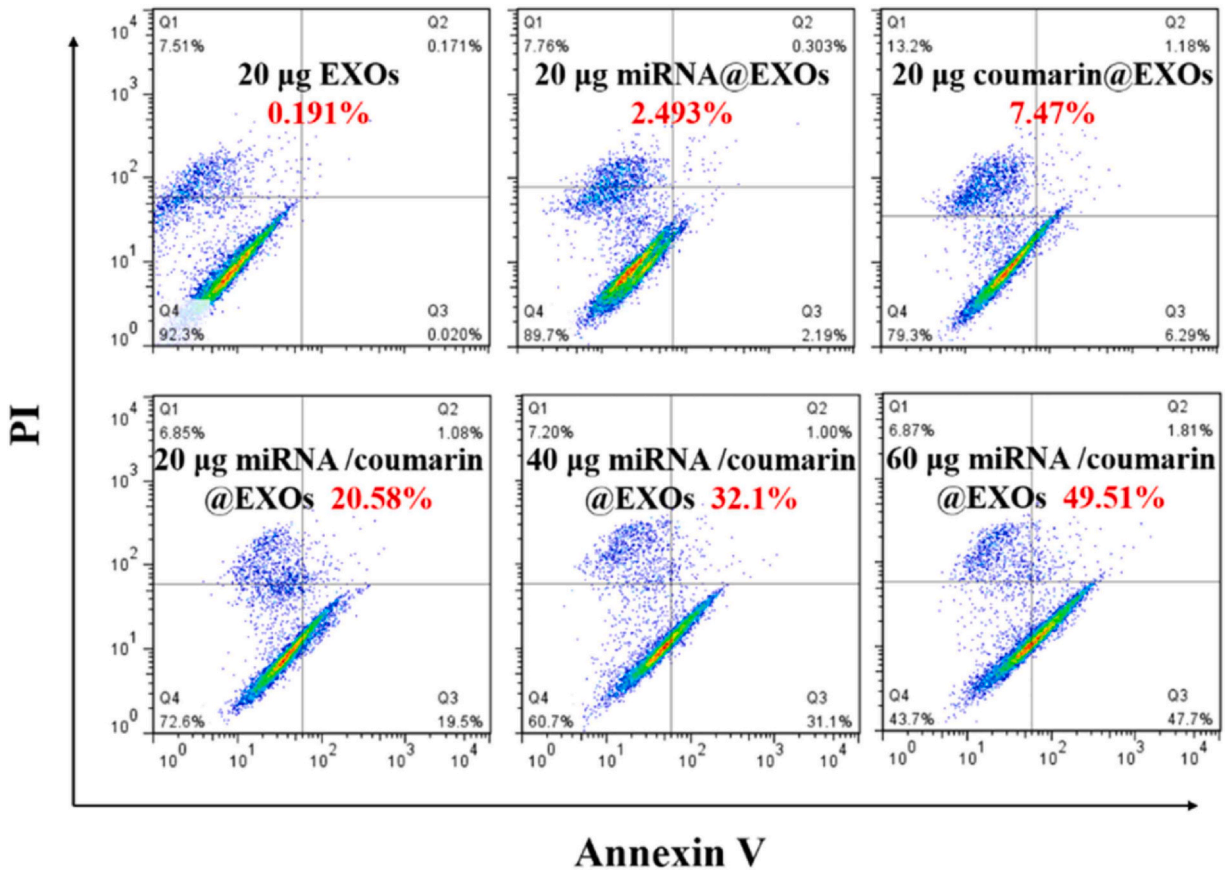

Fig. 4. Annexin V-FITC/PI analysis of the apoptosis of SKOV-3 cells after treatment with different materials at different concentrations. The statistically compared percentage of apoptotic cells has been highlighted in red in each graph.

4. Conclusion

In this paper, we constructed an exosome-based drug delivery system internally encapsulated with anticancer drugs 7-coumarin and miRNA to achieve a synergistic anticancer effect on ovarian cancer. Using exosomes as drug carriers enhanced the cell-entering capability and the targeting of the drugs. By simultaneously regulating cell autophagy by miRNA and accelerating cell apoptosis by 7-coumarin, a significantly better therapeutic effect was achieved, demonstrating the synergistic effect of the two drugs. Therefore, this study proposed a new exosome-based drug delivery strategy for anti-cancer therapy, which showed promising prospects for in vitro and clinical applications.

CRediT authorship contribution statement

Qian Zhu: Writing – review & editing, Data curation. **Sisi Zhou:** Supervision. **Quan Li:** Supervision. **Songqin Liu:** Writing – review & editing, Supervision, Funding acquisition, Conceptualization. **Xin Hua:** Writing – review & editing, Funding acquisition, Data curation, Conceptualization. **Yu Liu:** Writing – review & editing, Data curation. **Xi Liu:** Writing – original draft, Formal analysis, Data curation.

Declaration of Competing Interest

The authors declare that they have no known competing financial interests or personal relationships that could have appeared to influence the work reported in this paper.

Acknowledgments

This work was supported by the ZhiShan Scholar Program of Southeast University (2242022R40053).

Supporting information

The supplementary experimental details including the collection and analysis of exosomes, the construction of MNPs-CS, sample preparation for transmission electron microscopy and the nanoparticles tracking analysis. Supplementary figures for material characterizations, fluorescence spectra of the solutions before and after electroporation with drugs, flow cytometry analysis of different materials, flow cytometry analysis and CLSM images of IOSE80 cells after incubating with miRNA-FAM/7-coumarin@EXOs-MNPs for different time.

Appendix A. Supporting information

Supplementary data associated with this article can be found in the online version at doi:10.1016/j.bioana.2024.05.002.

References

[1] S. Benhadjeba, L. Edjekouane, K. Sauve, E. Carmona, A. Tremblay, Mol. Oncol. 12 (10) (2018) 1689–1705.
[2] M. Ewertz, C. Qvortrup, L. Eckhoff, Acta Oncol. 54 (5) (2015) 587–591.
[3] S.H. Chu, Y.J. Lee, E.S. Lee, Y. Geng, X.S. Wang, C.S. Cleeland, Support Care Cancer 23 (2) (2015) 513–524.
[4] H. Nie, X. Xie, D. Zhang, Y. Zhou, B. Li, F. Li, F. Li, Y. Cheng, H. Mei, H. Meng, L. Jia, Nanoscale 12 (2) (2020) 877–887.
[5] Y. Ji, J. Ji, H. Yin, X. Chen, P. Zhao, H. Lu, T. Wang, Bioengineered 12 (2) (2021) 12148–12156.
[6] Y. Fan, X. Duan, M. Zhao, X. Wei, J. Wu, W. Chen, P. Liu, W. Cheng, Q. Cheng, S. Ding, Biosens. Bioelectron. 154 (2020) 112066.
[7] Y. Liang, L. Duan, J. Lu, J. Xia, Theranostics 11 (7) (2021) 3183–3195.
[8] Y. Liang, X. Xu, X. Li, J. Xiong, B. Li, L. Duan, D. Wang, J. Xia, ACS Appl. Mater. Interfaces 12 (33) (2020) 36938–36947.
[9] Y. Liang, Z. Iqbal, J. Lu, J. Wang, H. Zhang, X. Chen, L. Duan, J. Xia, Mol. Ther. 31 (5) (2023) 1207–1224.
[10] X. Xu, Z. Iqbal, L. Xu, C. Wen, L. Duan, J. Xia, N. Yang, Y. Zhang, Y. Liang, Psychiatry Clin. Neurosci. 78 (2) (2024) 83–96.
[11] P. Vader, E.A. Mol, G. Pasterkamp, R.M. Schiffelers, Adv. Drug Deliv. Rev. 106 (Pt A) (2016) 148–156.
[12] C. Chen, Y. Li, Q. Wang, N. Cai, L. Wu, X. Yan, Anal. Bioanal. Chem. (2022).
[13] S. Ohno, M. Takanashi, K. Sudo, S. Ueda, A. Ishikawa, N. Matsuyama, K. Fujita, T. Mizutani, T. Ohgi, T. Ochiya, N. Gotoh, M. Kuroda, Mol. Ther. 21 (1) (2013) 185–191.
[14] M. Katakowski, B. Buller, X. Zheng, Y. Lu, T. Rogers, O. Osobamiro, W. Shu, F. Jiang, M. Chopp, Cancer Lett. 335 (1) (2013) 201–204.
[15] J. Du, Z. Wan, C. Wang, F. Lu, M. Wei, D. Wang, Q. Hao, Theranostics 11 (17) (2021) 8185–8196.
[16] A. Yuan, L. Ruan, R. Jia, X. Wang, L. Wu, J. Cao, X. Qi, Y. Wei, S. Shen, ACS Appl. Nano Mater. 5 (1) (2021) 996–1002.
[17] O.C.L.R. Farokhzad, ACS Nano 3 (2009) 16–20.
[18] D.D. Mosser, A.W. Caron, L. Bourget, C. Denis-Larose, B. Massie, Mol. Cell. Biol. 17 (9) (1997) 5317–5327.
[19] S. Fulda, Front. Oncol. 7 (2017) 128–131.
[20] C.W. Yun, S.H. Lee, Int. J. Mol. Sci. 19 (11) (2018) 3466–3483.
[21] A.V. Onorati, M. Dyczynski, R. Ojha, R.K. Amaravadi, Cancer 124 (16) (2018) 3307–3318.
[22] J.M. Mulcahy Levy, S. Zahedi, A.M. Griesinger, A. Morin, K.D. Davies, D.L. Aisner, B.K. Kleinschmidt-DeMasters, B.E. Fitzwalter, M.L. Goodall, J. Thorburn, V. Amani, A.M. Donson, D.K. Birks, D.M. Mirsky, T.C. Hankinson, M.H. Handler, A.L. Green, R. Vibhakar, N.K. Foreman, A. Thorburn, Elife 6 (2017).
[23] J.M. Levy, J.C. Thompson, A.M. Griesinger, V. Amani, A.M. Donson, D.K. Birks, M.J. Morgan, D.M. Mirsky, M.H. Handler, N.K. Foreman, A. Thorburn, Cancer Discov. 4 (7) (2014) 773–780.
[24] Y.P. Yang, L.F. Hu, H.F. Zheng, C.J. Mao, W.D. Hu, K.P. Xiong, F. Wang, C.F. Liu, Acta Pharm. Sin. 34 (5) (2013) 625–635.
[25] B. E, R. S, S. J, Neurosurg. Focus 14 (2) (2003) 1–6.
[26] E. Briceno, A. Calderon, J. Sotelo, Surg. Neurol. 67 (4) (2007) 388–391.
[27] Ann. Intern. Med., vol. 144(no. 5), 2006, pp. 337–43.
[28] J.M. Levy, A. Thorburn, Pharm. Ther. 131 (1) (2011) 130–141.
[29] X. Wang, H. Zhang, H. Yang, M. Bai, T. Ning, S. Li, J. Li, T. Deng, G. Ying, Y. Ba, Curr. Cancer Drug Targets 18 (4) (2018) 347–354.
[30] P. Vader, E.A. Mol, G. Pasterkamp, R.M. Schiffelers, Adv. Drug Deliv. Rev. 106 (2016) 148–156.
[31] J. Wen, S. Yeo, C. Wang, S. Chen, S. Sun, M.A. Haas, W. Tu, F. Jin, J.L. Guan, Breast Cancer Res. Treat. 149 (3) (2015) 619–629.
[32] R. Sun, S. Shen, Y.J. Zhang, C.F. Xu, Z.T. Cao, L.P. Wen, J. Wang, Biomaterials 103 (2016) 44–55.